International Journal for Multidisciplinary Research (IJFMR)
E-ISSN: 2582-2160 ● Website: www.ijfmr.com ● Email: editor@ijfmr.com

Synthesis of Niobium Pentoxide and its Reduced Graphene Oxide Nanocomposite for Enhanced Supercapacitor Applications

Vinuth Raj T N[1], Priya A Hoskeri[2]

[1]Department of Physics, Faculty of Engineering and Technology, Jain Deemed-to be University, Bangalore,562 112, India.
[2]Department of Physics, Dayananda Sagar College of Engineering, Kumarswamy Layout, Bangalore, 560 111, India.

Abstract

A simple hydrothermal synthetic route has been developed for the synthesis of perovskite lanthanum aluminate (Nb_2O_5) and reduced graphene oxide composite (RGO). The synthesized materials have been characterized for its morphology using, XRD, SEM, techniques. The materials are used as electrode materials for supercapacitor applications. Electron microscopic images indicate RGO sheets are densely attached to surface of Nb_2O_5 with perforated cage like morphology. A high specific capacitance of 751 Fg^{-1} at a scan rate of 2 mVs^{-1} was exhibited by RGO/ Nb_2O_5 hybrid structure electrode when compared to pure RGO (535 Fg^{-1}) and pure Nb_2O_{53} (175 Fg^{-1}) electrodes at the same scan rate using cyclic voltammetry (CV). By using chronopotentiometry (CP), the RGO/ Nb_2O_5 hybrid structure electrode out stretched specific capacitance of 572 Fg^{-1} at a current density of 0.5 Ag^{-1} and able to retain specific capacitance (C_{sp}) of about 427 Fg^{-1} even at very high current density of 10 Ag^{-1}.RGO/ Nb_2O_5 composite also possesses an energy density of 179 Wh kg^{-1} with a maximum power density of 1500 W kg^{-1}. From the Electrochemical Impedance Spectroscopy (EIS), the RGO/ Nb_2O_5 hybrid structure electrode has shown phase angle close to -90^o for frequency up to 0.01Hz, suggesting that the nanocomposite electrode material approached ideal capacitor behavior.

Keywords: RGO-Nb_2O_5 composites; Hydrothermal synthesis; Supercapacitors.

1. Introduction

The supercapacitor, also known as the electrochemical capacitor, is a new type of energy storage device that sits between conventional capacitors and batteries. Due to the high power density, fast charging and discharging time, long cycle life, and wide operating temperature range, etc.[1,2], supercapacitor has shown great potential in application as energy storage and supply green transportation, mobile power, wearable smart devices, military special equipment, long-distance telecommunication, and other new industrialization fields [3–5], which greatly promotes basic energy science research and enormous economic development.

Depending on their energy storage principle, supercapacitors can be categorized as either faradaic pseudocapacitor or electric double layer capacitor. Due to their superior density and power density, electrochemical capacitors outperform conventional electrostatic capacitors and batteries in terms of

performance. The basic principle of electric double layer capacitors is that carbon-based materials store electrical energy at the electrode-electrolyte interface, whereas multivalent transition metal oxides and conducting polymers that can undergo redox reaction in electrolytes exhibit faradaic pseudocapacitance [6,7].

Typically, supercapacitor assemblies consist of four components: the couple electrodes, electrolyte, a current collector, and a separator, with the electrode being the determining factor for the capacitor's primary performance. Therefore, low-resistance electrode materials are required to reduce energy loss during the charging and discharging processes [8,9]. The electrode materials must simultaneously possess physicochemical stability, good performance of charge capacity, exceptional specific capacitance values, and outstanding anti-fatigue performance. Although carbon-based materials are common capacitive materials, conductive polymers and metal oxides [10,11] have been thoroughly investigated. However, these single materials do not meet the requirements for the development of new, superior energy storage materials, particularly the materials required for the development of high-performance supercapacitors [12,13].

Since its discovery, graphene has been studied extensively as a supercapacitor's carrier material due to its high specific surface area, high electrical conductivity, and good chemical and mechanical stability. Utilizing a single graphene material for energy storage is neither ineffective nor wasteful. Consequently, research into capacitive materials is crucial [14,15]. It improves the performance of graphene by combining two-dimensional graphene with other materials, such as transition metal oxides, hydroxides, conductive polymers, sulphides, and polymer compounds, in order to obtain an excellent composite via chemical group doping and surface defect modification. It has been reported that RuO2, Co3O4, Ni(OH)2, CoS2, and other materials can be combined with graphene [16–18]. Niobium pentachloride is a promising precursor among transition metal oxides and is easily converted into niobium pentoxide (Nb_2O_5). Nb_2O_5 has excellent acid and alkali corrosion resistance, a large number of active sites, excellent optical properties, and stable electrochemical properties, which have attracted increasing interest [19,20].

This paper describes the facile synthesis of RGO- Nb_2O_5 nanocomposites with excellent capacitance and stability. The nanocomposite of Nb_2O_5 and RGO significantly increases specific capacitance. Using cyclic voltammetry and galvanostatic current charge-discharge, the electrochemical properties of the RGO-Nb_2O_5 nanocomposite were analyzed and compared to those of pure Nb_2O_5 and RGO.

2. Materials and Methods

2.1 Synthesis

2.1.1 Synthesis of Graphene oxide

A modest modification to the hummer's approach was used to synthesis GO. It was decided to make a 9:3 mixture of H_2SO_4 and H_3PO_4. A second graphite/$KMnO_4$ mixture with a mass ratio of 2:6 was made. To avoid a vigorous reaction, the acid mixture was slowly poured into the beaker containing the graphite-$KMnO_4$ mixture in an ice bath at a temperature of 5 to 10 °C. The solution was kept at a constant temperature of 60 °C in a water bath. The heated, somewhat dark solution was withdrawn from the water bath and mixed with 400 mL distilled cold water to end the reaction. After that, 5 mL of H_2O_2 was added dropwise, resulting in a yellowish-colored solution. The addition of H_2O_2 was intended to terminate the oxidation reaction by reacting directly with the excess potassium permanganate. The

reaction product was rinsed four times with HCl aqueous solution and distilled water until it reached the appropriate pH.[19]

2.1.2 Conversion of GO-RGO

Graphene oxide (GO) was synthesized from natural graphite flakes using a modified Hummers method. To prepare a suspension of GO, 0.3 mg/mL of graphene oxide was dispersed in deionized (DI) water. The reduction of GO was then carried out by adding green tea extract (GTE) to the GO suspension in a batch reactor-closed system. Typically, GTE was added at a weight ratio of GTE/GO=1, with 30 mL of GO suspension. The reduction reaction took place in the reactor for 8 hours at a temperature of 90 °C. Throughout the reduction process, the GO-GTE mixture was continuously stirred at a speed of 200 rpm. After the reaction, the suspension containing the final product was filtered using a nylon membrane with a pore size of 0.22 µm. The collected material was washed 3-5 times with DI water. The resulting product was named Reduced Graphene Oxide (RGO)[20].

2.1.3 Synthesis of RGO-Nb_2O_5 Nanocomposite

2.1.3.1 Synthesis of Niobium pentoxide

Niobium pentoxide can be synthesized through a precipitation method. Initially, a niobium-containing precursor, such as niobium chloride or niobium oxalate, is dissolved in a suitable solvent, typically water or an organic solvent. The solution is then subjected to precipitation by adding a precipitating agent, such as ammonium hydroxide or sodium hydroxide, to form niobium hydroxide. The obtained niobium hydroxide precipitate is further washed with water to remove any impurities and then dried. Subsequently, the dried niobium hydroxide is subjected to calcination at a high temperature, typically around 600-800 °C, in a furnace. This thermal treatment leads to the conversion of niobium hydroxide into niobium pentoxide. The resulting niobium pentoxide is then cooled, collected, and stored for further use.

2.1.3.2 Synthesis of RGO-Nb_2O_5

To synthesize RGO-Nb_2O_5, start by preparing graphene oxide (GO) using the modified Hummers method. Next, exfoliate the GO by sonicating it in water or a suitable solvent to obtain reduced graphene oxide (RGO) sheets [21]. Then, mix the RGO sheets and Nb_2O_5 nanoparticles in a solvent, such as ethanol or water, and sonicate the mixture to ensure a homogeneous dispersion. Subsequently, perform a hydrothermal treatment under controlled temperature and pressure conditions to promote the growth and deposition of Nb_2O_5 onto the RGO surface. This process allows for the formation of RGO-Nb_2O_5 composite material. Finally, wash the obtained composite, followed by drying and calcination to remove any residual solvents or organic species, resulting in the final RGO-Nb2O5 composite material ready for characterization and subsequent applications.

2.1.4 working electrode preparation.

The flower petals like RGO-Nb_2O_5 composite, pure RGO and pure Nb_2O_5 were used in a standard technique for fabricating the working electrode for capacitance measurements. The composition of the working electrodes was 85 wt% RGO-Nb_2O_5, 10 wt% acetylene black, and 5 % polytetrafluoroethylene (PTFE) in 1 -methyl-2-pyrrolidinone (NMP). A small amount of IPA was added to the mixture to fully mix and grind it into a homogeneous slurry. Then, 10 pieces of carbon paper with an average area of 1.0 cm 1.0 cm were uniformly coated with the prepared slurry. The solid electrodes were then dried using a vacuum oven equipped with a pressure gauge for 8 hours at 60 °C. The average amount of active

materials in 10 electrodes is used to calculate the loading mass in each electrode. A working electrode, counter electrode (Pt wire), and reference electrode (calomel) were used in a three-electrode setup for the electrochemical performance, which was carried out in 6.0 M KOH. It has been used to conduct electrochemical tests on the CHI-660E workstation.[21]

2.3 Material characterization

Bruker D2 Phaser XRD tools were used to obtain X-ray diffraction (XRD) patterns. A scanning electron microscope was used to analyze the surface morphology (SEM) (JEOL JSM 840A)

2.3.1 SEM Analysis

The SEM image of the pure Nb_2O_5 particles shows irregular shapes petals of flower on the surface of the layers of reduced graphene oxide (RGO) were represented in figure.1 A &B. The merged particles of the pure Nb_2O_5 particles indicated in the figure. 1 C.

Figure 1: A, 1 B and 1 C- SEM Images of RGO-Nb_2O_5

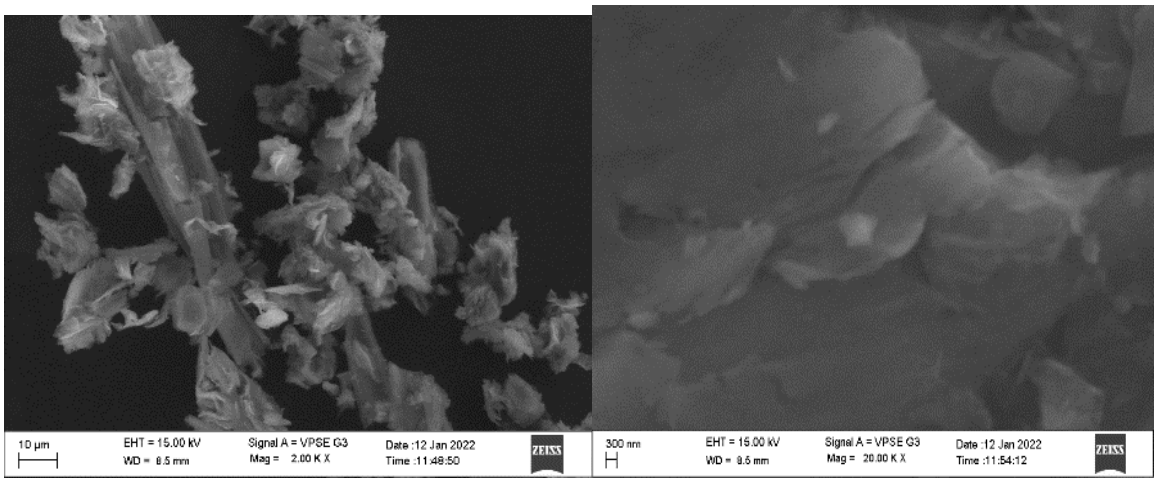

Figure 1 A Figure 1 B

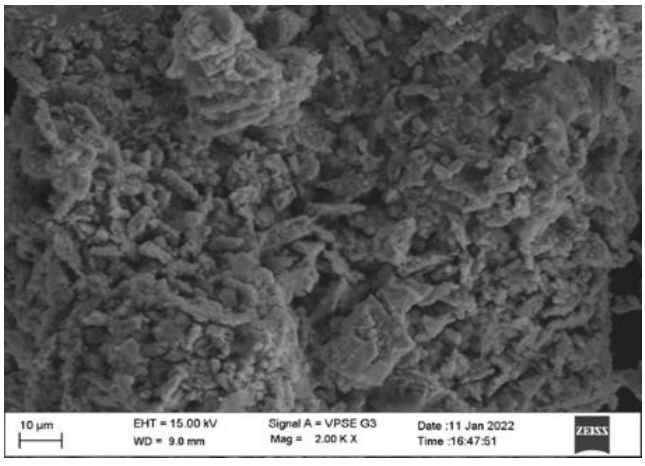

Figure 1 C

2.3.2 XRD Analysis

Figure 2: XRD image of RGO-Nb_2O_5

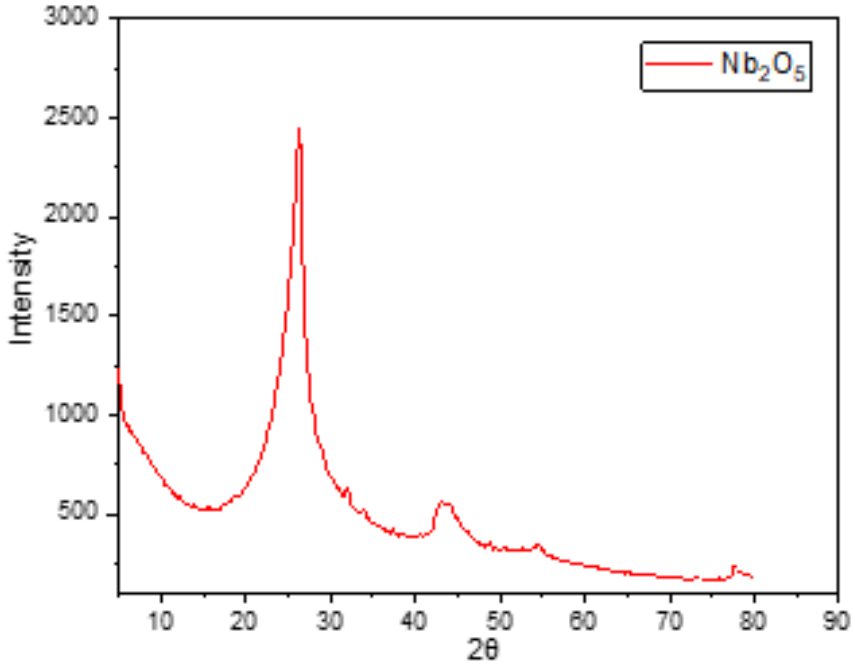

Figure 2 shows the X-ray diffractogram of the RGO-Nb_2O_5 composites. Diffractogram of the composites shows the asymmetric diffraction pattern is due to the RGO at $2\theta \approx 25°$ which relates to the (002) regular hump of the graphene, other distinct peak patterns of pure Nb_2O_5 has very good agreement with the orthorhombic Nb_2O_5 (JCPDS-37-1468) from the literature. It also indicates the peaks at 26.5°, 34.58°, 37.60°, 43.52°, 52.46°, 54.44° were assigned to pure Nb_2O_5, this gives an evidence to possible that the Nb_2O_5 crystals particles adhering to the graphene sheets.

2.4 Supercapacitors Applications

2.4.1 Cyclic Voltammetry Studies

Cyclic voltagramm of the pure RGO, pure Nb_2O_5 and developed RGO-Nb_2O_5 composites were analysed in an aqueous 3 M KOH electrolyte was shown in the Figure3 and working potential window between -0.3 V to 1.2 V. The CV of the composite indicates the pervert rectangular shape and obtained a larger specific capacitance (C_{sp}) of 440 F/g than the pure RGO (354 F/g) and pure Nb_2O_5(110 F/g). In CV curves of the material observed the characteristic redox peaks at 0.43 V (Cathodic) and 0.21 V (anodic), which involves the pseudocapacitive behaviour of the composite is due to the faradic redox reactions of the +5 and +4 of the Nb [22,23].

$$\mathbf{K^+ + e^- + Nb_2O_5 \leftrightarrow KNb^{+4}Nb^{+5}O_5} \qquad \textbf{(i)}$$

Figure 3: CV curves of RGO-Nb_2O_5 composites, pure RGO and pure Nb_2O_5 electrode materials at a scan rates of 50 mV/s.

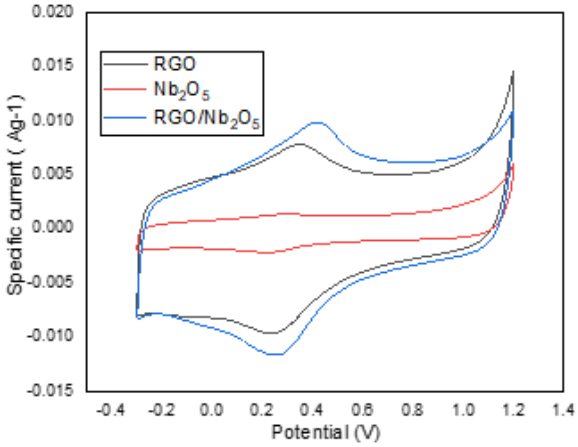

The specific capacitance (C_{sp}) was calculated using the following equation.

$$C_{sp} = \frac{1}{\gamma W(\Delta V)} \int_{V_D}^{V_C} iVdV \quad (1)$$

Where represents the scan rate (mVs^{-1}), W represents the active mass of the material (g), and V represents the potential window (V). All of the capacitance values determined for each electrode are displayed in Table 1. The CV behaviour of the composite were conducted by variation of different scan rate in the range of 2 – 100 mVs^{-1} can be observed in the Figure 4. C_{sp} data at lower scan rate is 751 Fg^{-1} is may due to the more interaction between the active material and electrolyte, this goes on decreasing as increases in the scan rate of CV studies which implies that at higher scan rate produces C_{sp} of 397 Fg^{-1}. The significant improvement in the capacitance behaviour of the composite material is may due to the redox nature of the Nb were aligned on the surface of RGO, which enhances the capacitance through improving catalytic activity. The comparison of the electrode materials was carried out shown in the Figure 5, its corresponding C_{sp} values are tabulated in Table 1.

Figure 4: CV curves at different scan rates for RGO-Nb_2O_5 nanocomposites electrode.

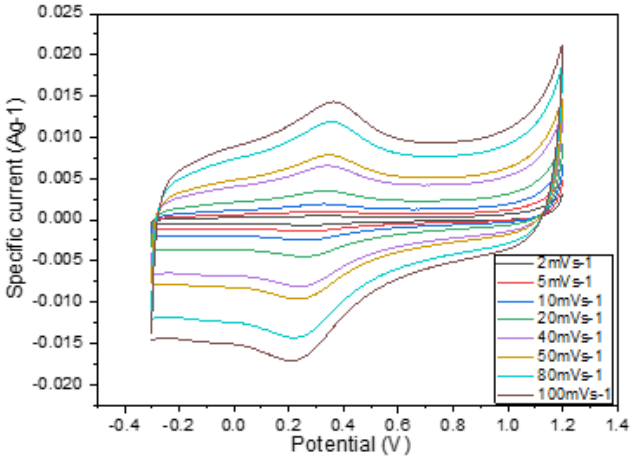

Figure 5: Specific capacitance RGO-Nb_2O_5 nanocomposites, pure RGO and pure Nb_2O_5 electrodes as a function of scan rates.

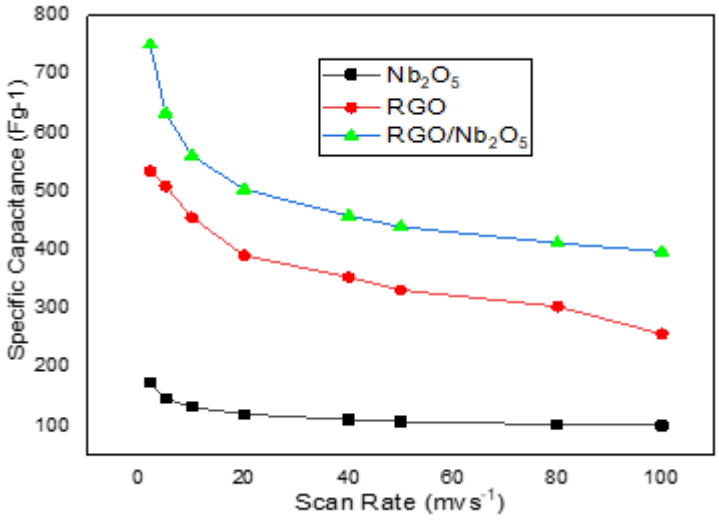

2.4.2 Galvanostatic charge discharge studies (GCD)

Figure 6: Comparison of GCD curves of RGO-Nb_2O_5 nanocomposites, pure RGO and pure Nb_2O_5 electrodes at constant current density of 2.5 mA.

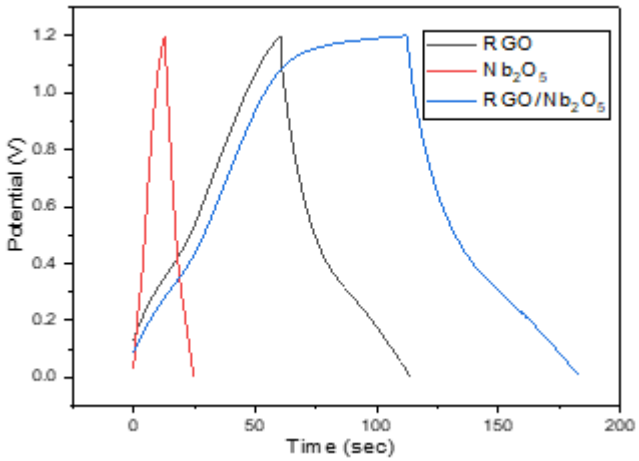

Figure 7: Charge/discharge curves of RGO-Nb_2O_5 nanocomposites at different current density.

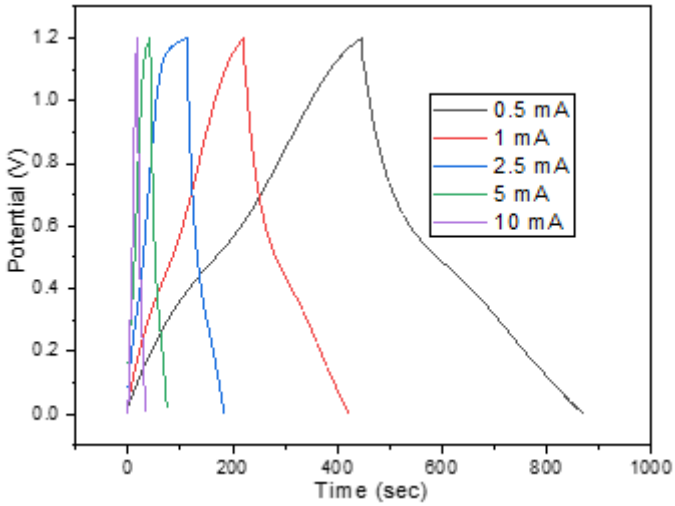

Figure 8: Variation of specific capacitance as a function of various current densities for RGO-Nb_2O_5 composites, pure RGO and pure Nb_2O_5 electrodes

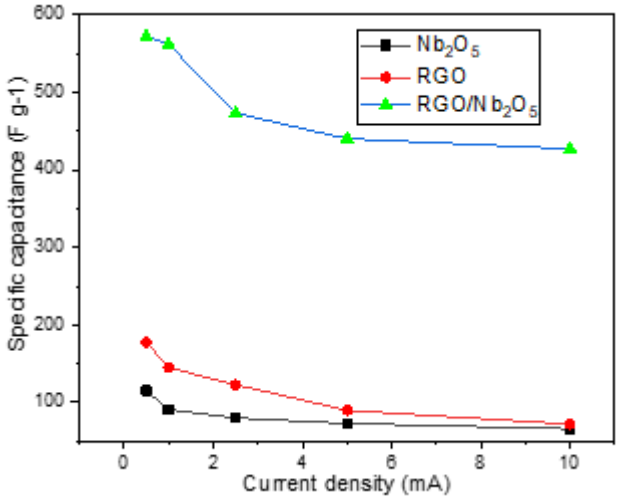

Table. 1 Specific capacitance of RGO-Nb_2O_5 nanocomposites, pure RGO and pure Nb_2O_5 electrodes using CV at different scan rates and CP at different current densities.

Sl. no	Scan rate (mVs^{-1})	Specific capacitance (C_{sp})			Current density (Ag^{-1})	Specific capacitance (C_{sp})		
		RGO- Nb_2O_5 composite	Pure RGO	Pure Nb_2O_5		RGO-Nb_2O_5 composites	Pure RGO	Pure Nb_2O_5
1	2	**751**	535	175	-	-	-	-
2	5	**634**	509	147	0.5	**572**	178	115
3	10	**561**	456	132	1.0	**562**	145	91
4	20	**503**	391	120	2.5	**473**	123	80
5	40	**458**	354	110	5.0	**440**	90	73
6	50	**440**	332	107	10	**427**	72	66
7	80	**412**	304	102	-	-	-	-
8	100	**397**	257	100	-	-	-	-

Later, the galvanostatic charge-discharge (GCD) test gives an idea about how improvement in the energy storage of RGO-Nb_2O_5 composites by addition of Nb_2O_5 to RGO. The GCD studies were performed in the potential window of 0.0-1.2 V for RGO-Nb_2O_5 composites, pure RGO and pure Nb_2O_5 electrodes. At 2.5 mA/cm^2, compared the RGO-Nb_2O_5 composites, pure RGO and pure Nb_2O_5 electrodes, which produces corresponding C_{sp} values 473, 123 and 73 Fg^{-1} respectively. It is due to the RGO-Nb_2O_5 composites shows higher the integral area and higher the discharge time was observed in the **Figure 6** than that of the individuals. For composite, GCD studies were continued at different current densities from 0.5 to10 mA cm^{-2} (**Figure 7**), which produces C_{sp} of 575 Fg^{-1} (0.5 mA cm^{-2}) and 427 F/g

(10 mA cm^{-2}). The higher the C_{sp} value at lower current density is due to the higher the rate of electron diffusion with the electrode materials and electrolyte, at higher current density decreases in the C_{sp} value because of the rapid kinetics in the chemical reactions. A considerable retention of the composite electrode was satisfactory, which shows the 74.65% of Cs retention at 20 times of current density (10mA cm^{-2}) and best C_{sp} values were obtained than the pure RGO and pure Nb_2O_5 electrodes were shown in **Figure 8**. On the basis of charge/discharge curves, specific capacitance of electrodes was calculated using the equation (2) depicted in **Table 1.**

$$C_{sp} = \frac{i}{W \times \frac{\Delta V}{\Delta t}} \quad (2)$$

where I represents the current (A), t represents the discharge time (s), V represents the potential window (V), and W represents the mass of the electroactive materials (g).

Further the all electrode materials were evaluated to check its energy density and power density, the RGO-Nb_2O_5 composites show an appreciable value than individuals. using equations (3) and (4), the energy density (ED) and power density (PD) of electrodes were calculated.

$$E = \frac{1}{2}CV^2 \quad (3)$$

$$P = \frac{E}{t} \quad (4)$$

Where E is the energy density ($Whkg^{-1}$), V is the potential window (V), C is the specific capacitance (Fg^{-1}), t is the discharge time (s), and P is the power density (Wkg^{-1}). In **Table 2**, the calculated ED and PD of all electrode systems are tabulated. The composite active material electrode complete discharges and produces an ED of 179 Wh kg^{-1} and PD 1500 W/kg at 0.5 Ag^{-1}. As the increase in the applied current density the PD also increases and RGO-Nb_2O_5 composites are produced 30 kW kg^{-1}, which is characteristic best values on compare with the pure RGO and pure Nb_2O_5**.**

Table 2: Calculated ED and PD values of RGO-Nb_2O_5 nanocomposites, pure RGO and pure Nb_2O_5 electrodes using CP data.

Sl. No.	Current density (Ag^{-1})	RGO-Nb_2O_5 nanocomposites		Pure RGO		Pure Nb_2O_5	
		ED ($Whkg^{-1}$)	PD (Wkg^{-1})	ED ($Whkg^{-1}$)	PD (Wkg^{-1})	ED ($Whkg^{-1}$)	PD (Wkg^{-1})
1	0.5	179	1500	36	566	36	1500
2	1	176	3000	29	1135	28	3000
3	2.5	148	7500	25	2857	25	7500
4	5	137	15000	18	5635	23	15000
5	10	133	30000	14	11520	21	30000

Figure 9: Ragone plot of RGO-Nb_2O_5 nanocomposites, pure RGO and pure Nb_2O_5 electrodes.

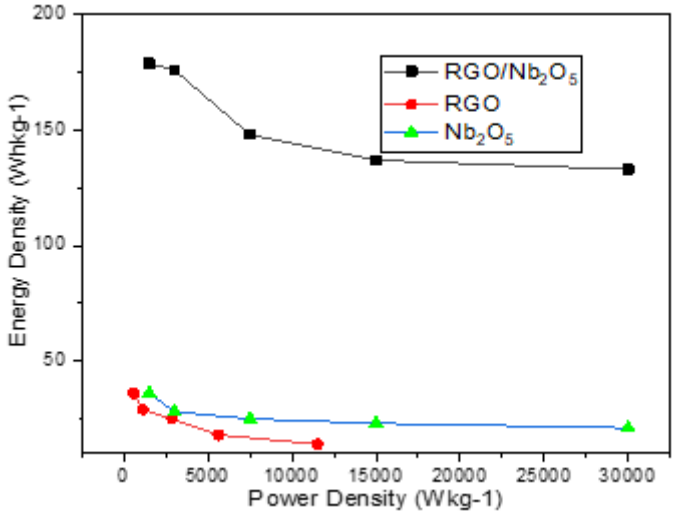

2.4.3 Galvanostatic charge discharge studies (GCD)

EIS testing has been carried out on the electrodes between 0.01 and 10^5 Hz. The Nyquist plot R_{ct} and R_s values were calculated using the equivalent circuit shown in **Figure 10**. The electrodes provided values

of R_s and R_{ct} that were estimated. The Nyquist plots high frequency region showed low resistance, which is useful for charge-discharge cycle analysis and power density. It is due to electrodes are possesses good capacitive and low diffusion resistances, a low frequency area Nyquist plot that is roughly parallel to the imaginary axis was found in the composites, this produces the supporting evidence to the CV and GCD analysis of the composites.

Figure 10: The Nyquist plots of RGO-Nb_2O_5 nanocomposites, pure RGO and pure Nb_2O_5 electrodes.

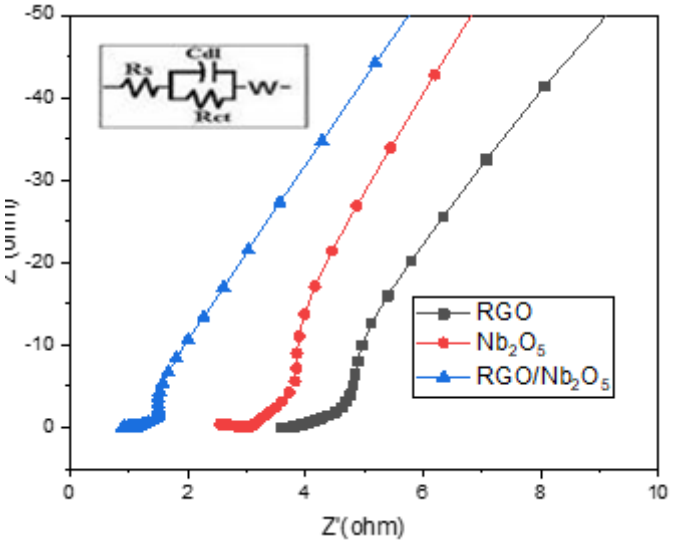

Figure 11: Bode plots of RGO-Nb_2O_5 composites, pure RGO and pure Nb_2O_5 electrodes.

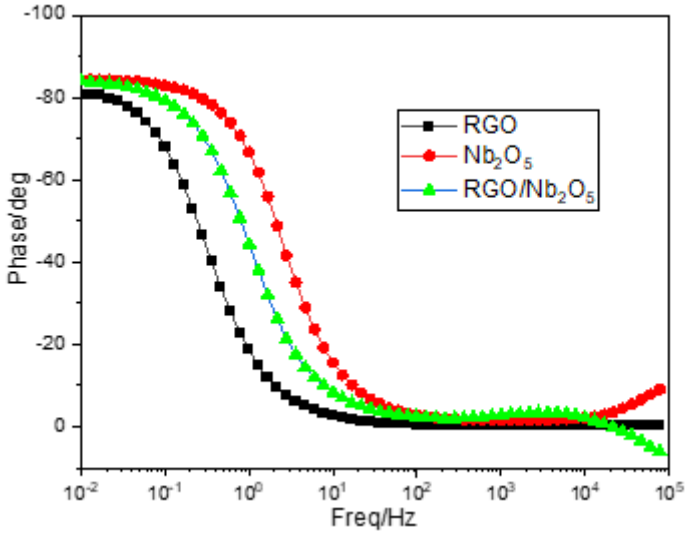

As shown in Figure11, the pseudo-capacitive property of the composite material is represented by the Bode plot, which has a lower frequency than that of the ideal capacitor. The composite shows low frequency denotes even spreading of Nb particles on the surface of RGO layers, which results in improved conductivity in composites than the pure RGO and Pure Nb. From the Electrochemical Impedance Spectroscopy (EIS), the RGO/ Nb_2O_5 hybrid structure electrode has shown phase angle close to -90^o for frequency up to 0.01Hz, suggesting that the nanocomposite electrode material approached ideal capacitor behavior.

Figure 12: Retention ratio graph of RGO-Nb_2O_5 nanocomposites, pure RGO and pure Nb_2O_5 electrodes.

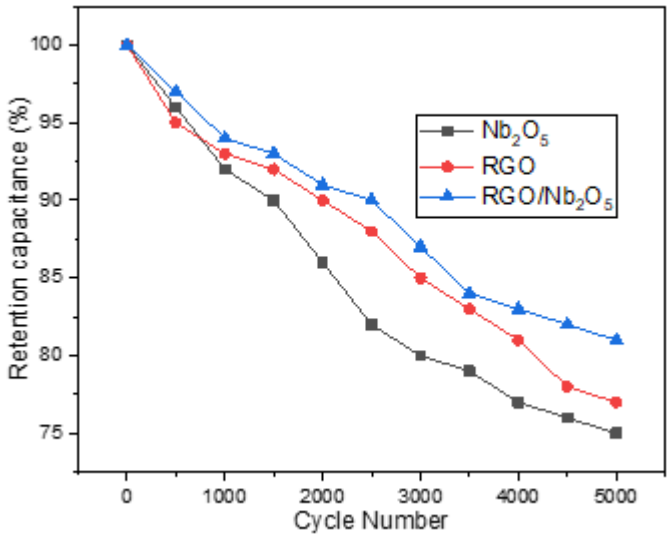

s

In **Figure 12**, the cyclic performance of the electrode materials was exhibited, among those composite electrode produces best retention values. All the electrodes show decreasing Cs values in the interval of every 500 cycles, in each interval the composite electrode show better by exhibiting higher Cs value. In

the 5K cyclic performance, the RGO-Nb_2O_5 electrode Cs retention was 83% and that of Pure Nb_2O_5 was 76 %.

2.5 Conclusions

Using a simple hydrothermal technique, Nb_2O_5 nanoparticles are firmly anchored on nitrogen-doped RGO and used as an electrode material for its electrochemical performance in supercapacitor applications. In comparison to pure Nb_2O_5 and RGO, the electrochemical performance of Nb_2O_5 anchored on RGO was superior. The RGO-Nb_2O_5 nanocomposite demonstrated a high energy density of 179 Wh kg^{-1} at a power density of 1500 W kg^{-1} and was able to maintain an energy density of 133 Wh kg^{-1} even at a power density of 30000 W kg^{-1}. Additional work on the fabrication of an asymmetric device using RGO-Nb_2O_5 nanocomposite could pave the way for future energy storage research utilizing Niobium-related materials.

References

1. A.N. Naveen, S. Selladurai, "Novel synthesis of highly porous three-dimensional nickel cobaltite for supercapacitor application", Ionics (Kiel). 22 (2016) 1471–1483. https://doi.org/10.1007/s11581-016-1664-7.
2. K. Zhang, X. Zhang, W. He, W. Xu, G. Xu, X. Yi, X. Yang, J. Zhu, "Rational design and kinetics study of flexible sodium-ion full batteries based on binder-free composite film electrodes", J. Mater. Chem. A. 7 (2019) 9890–9902. https://doi.org/10.1039/c9ta01026b.
3. Y. Hui, Y. Shewen, W. Yunfeng, Z. Jiaming, J. Jingwen, C. Jiahao, Z. Qinqin, L. Tongxiang, "Scalable production of hierarchical N-doping porous carbon@Cu composite fiber based on rapid gelling strategy for high-performance supercapacitor", J. Alloys Compd. 792 (2019) 976–982. https://doi.org/10.1016/j.jallcom.2019.04.138.
4. H. Yang, S. Ye, J. Zhou, T. Liang, "Biomass-derived porous carbon materials for supercapacitor", Front. Chem. 7 (2019). https://doi.org/10.3389/fchem.2019.00274.
5. A.S. Aricò, P. Bruce, B. Scrosati, J.-M. Tarascon, W. Van Schalkwijk, "Nanostructured materials for advanced energy conversion and storage devices", Nat. Mater. 4 (2010) 148–159. www.nature.com/naturematerials.
6. V. Augustyn, P. Simon, B. Dunn, "Pseudocapacitive oxide materials for high-rate electrochemical energy storage", Energy Environ. Sci. 7 (2014) 1597–1614. https://doi.org/10.1039/c3ee44164d.
7. Z. Guo, E. Takeuchi, "Best Practices for Reporting on Energy Storage", ACS Appl. Mater. Interfaces. 7 (2015) 16131–16132. https://doi.org/10.1021/acsami.5b06029.
8. W. Hu, W. Zhang, Y. Wu, W. Qu, "Self-assembly and hydrothermal technique syntheized Fe2O3-RGO nanocomposite: The enhancement effect of electrochemical simultaneous detection of honokiol and magnolol", J. Electroceramics. 40 (2018) 1–10. https://doi.org/10.1007/s10832-017-0075-0.
9. T.N. Vinuth Raj, P.A. Hoskeri, H.B. Muralidhara, B.P. Prasanna, K. Yogesh Kumar, F.A. Alharthi, M.S. Raghu, "Tantalum pentoxide functionalized nitrogen-doped reduced graphene oxide as a competent electrode material for enhanced specific capacitance in a hybrid supercapacitor device", J. Alloys Compd. 861 (2021) 158572. https://doi.org/https://doi.org/10.1016/j.jallcom.2020.158572.
10. A. Khataee, R.D.C. Soltani, Y. Hanifehpour, M. Safarpour, H. Gholipour Ranjbar, S.W. Joo, "Synthesis and characterization of dysprosium-doped ZnO nanoparticles for photocatalysis of a textile dye under visible light irradiation", Ind. Eng. Chem. Res. 53 (2014) 1924–1932.

https://doi.org/10.1021/ie402743u.

11. L. Kong, C. Zhang, J. Wang, W. Qiao, L. Ling, D. Long, "Free-Standing T-Nb2O5/Graphene Composite Papers with Ultrahigh Gravimetric/Volumetric Capacitance for Li-Ion Intercalation Pseudocapacitor", ACS Nano. 9 (2015) 11200–11208. https://doi.org/10.1021/acsnano.5b04737.
12. E. Lim, H. Kim, C. Jo, J. Chun, K. Ku, S. Kim, H.I. Lee, I.S. Nam, S. Yoon, K. Kang, J. Lee, J. Lee, "Advanced hybrid supercapacitor based on a mesoporous niobium pentoxide/carbon as high-performance anode", ACS Nano. 8 (2014) 8968–8978. https://doi.org/10.1021/nn501972w.
13. H. Mahdavi, P.K. Kahriz, H. Gholipour Ranjbar, T. Shahalizade, "Enhancing supercapacitive performance of polyaniline by interfacial copolymerization with melamine", J. Mater. Sci. Mater. Electron. 27 (2016) 7407–7414. https://doi.org/10.1007/s10854-016-4715-y.
14. H.R. Naderi, M. Reza Ganjali, P. Norouzi, "The study of supercapacitive stability of MnO2/MWCNT nanocomposite electrodes by fast fourier transformation continues cyclic voltammetry", Int. J. Electrochem. Sci. 11 (2016) 4267–4282. https://doi.org/10.20964/2016.06.60.
15. T.N. Vinuth Raj, P.A. Hoskeri, H.B. Muralidhara, C.R. Manjunatha, K. Yogesh Kumar, M.S. Raghu, "Facile synthesis of perovskite lanthanum aluminate and its green reduced graphene oxide composite for high performance supercapacitors", J. Electroanal. Chem. 858 (2020) 113830. https://doi.org/10.1016/j.jelechem.2020.113830.
16. G. He, M. Qiao, W. Li, Y. Lu, T. Zhao, R. Zou, B. Li, J.A. Darr, J. Hu, M.M. Titirici, I.P. Parkin, S, "N-Co-Doped Graphene-Nickel Cobalt Sulfide Aerogel: Improved Energy Storage and Electrocatalytic Performance", Adv. Sci. 4 (2017) 1600214. https://doi.org/10.1002/advs.201600214.
17. I. Nowak, M. Ziolek, "Niobium compounds: preparation, characterization, and application in heterogeneous catalysis", Chem. Rev. 99 (1999) 3603–3624. https://doi.org/10.1021/cr9800208.
18. B. Orel, M. Maček, J. Grdadolnik, A. Meden, "In situ UV-Vis and ex situ IR spectroelectrochemical investigations of amorphous and crystalline electrochromic Nb2O5 films in charged/discharged states", J. Solid State Electrochem. 2 (1998) 221–236. https://doi.org/10.1007/s100080050092.
19. K. Qin, J. Kang, J. Li, C. Shi, Y. Li, Z. Qiao, N. Zhao, "Free-standing porous carbon nanofiber/ultrathin graphite hybrid for flexible solid-state supercapacitors", ACS Nano. 9 (2015) 481–487. https://doi.org/10.1021/nn505658u.
20. K. Saravanan, C.W. Mason, A. Rudola, K.H. Wong, P. Balaya, T"he first report on excellent cycling stability and superior rate capability of Na3V2(PO4)3 for sodium ion batteries", Adv. Energy Mater. 3 (2013) 444–450. https://doi.org/10.1002/aenm.201200803.
21. T.N. Vinuth Raj, P.A. Hoskeri, S. Hamzad, M.S. Anantha, C.M. Joseph, H.B. Muralidhara, K. Yogesh Kumar, F.A. Alharti, B.-H. Jeon, M.S. Raghu, "Moringa Oleifera leaf extract mediated synthesis of reduced graphene oxide-vanadium pentoxide nanocomposite for enhanced specific capacitance in supercapacitors", Inorg. Chem. Commun. 142 (2022) 109648. https://doi.org/https://doi.org/10.1016/j.inoche.2022.109648.
22. X. Wang, C. Yan, J. Yan, A. Sumboja, P.S. Lee, "Orthorhombic niobium oxide nanowires for next generation hybrid supercapacitor device", Nano Energy. 11 (2015) 765–772. https://doi.org/10.1016/j.nanoen.2014.11.020.
23. M. Wei, K. Wei, M. Ichihara, H. Zhou, "Nb2O5 nanobelts: A lithium intercalation host with large capacity and high rate capability", Electrochem. Commun. 10 (2008) 980–983. https://doi.org/10.1016/j.elecom.2008.04.031.